Reaction Mechanism of $HCN^+ + C_2H_4$: A Theoretical Study

Yan Li, Hui-ling Liu, Xu-ri Huang,* Dequan Wang, Chia-chung Sun, and Au-chin Tang

State Key Laboratory of Theoretical and Computational Chemistry, Institute of Theoretical Chemistry, Jilin University, Changchun 130023, People's Republic of China

Received: June 16, 2008; Revised Manuscript Received: September 4, 2008

The complex doublet potential energy surface for the ion−molecule reaction of HCN^+ with C_2H_4 is investigated at the B3LYP/6-311G(d,p) and CCSD(T)/6-311++G(3df,2pd) (single-point) levels. The initial association between HCN^+ and C_2H_4 forms three energy-rich addition intermediates, **1** ($HCNCH_2CH_2^+$), **2** (HC-c$NCH_2CH_2^+$), and **3** (N-c$CHCH_2CH_2^+$), which are predicted to undergo subsequent isomerization and decomposition steps. A total of nine kinds of dissociation products, including $\mathbf{P_1}$ ($HCN + C_2H_4^+$), $\mathbf{P_2}$ ($HCNCHCH_2^+ + H$), $\mathbf{P_3}$ ($NCCH_2 + CH_3^+$), $\mathbf{P_4}$ ($CN + C_2H_5^+$), $\mathbf{P_5}$ ($NCCHCH_2^+ + H_2$), $\mathbf{P_6}$ ($HNCCHCH_2^+ + H$), $\mathbf{P_7}$ (c-$CHCCH_2N^+ + H_2$), $\mathbf{P_8}$ (c-$NHCCH_2C^+ + H_2$), and $\mathbf{P_9}$ ($HNCCCH^+ + H_2 + H$), are obtained. Among the nine products, $\mathbf{P_1}$ is the most abundant product. $\mathbf{P_2}$ is the second feasible product but is much less competitive than $\mathbf{P_1}$. $\mathbf{P_3}$, $\mathbf{P_4}$, $\mathbf{P_5}$, and $\mathbf{P_6}$ may have the lowest yields observed. Other products, $\mathbf{P_7}$, $\mathbf{P_8}$, and $\mathbf{P_9}$, may become feasible at high temperature. Because the intermediates and transition states involved in the most favorable pathway all lie below the reactant, the $HCN^+ + C_2H_4$ reaction is expected to be rapid, which is confirmed by experiment. The present calculation results may provide a useful guide for understanding the mechanism of HCN^+ toward other unsaturated hydrocarbons.

1. Introduction

Titan, the largest satellite of Saturn, has attracted considerable interest because its atmosphere is so dense and because it is one of the places where the most complex atmospheric organic chemistry takes place in the solar system. A great deal of effort has been expended in describing the structure and the composition of Titan's atmosphere.[1−9] It has been established that Titan's dense and complex atmosphere is essentially composed of nitrogen and methane but also contains traces of hydrogen, ethane, ethylene, and acetylene.[10−12] Primary ionization begins in Titan's ionosphere both by photoionization from solar radiation and by impact ionization from magnetospheric electrons.[13−16] The reactions that occur via the primary ions N^+ and N_2^+ reacting with CH_4 initiate the ion-process, which yields the product ions CH_2^+, CH_3^+, CH_4^+, and HCN^+. The ions then react further with hydrocarbons that are present in abundance in Titan's atmosphere such as methane (CH_4), acetylene (C_2H_2), ethylene (C_2H_4), ethane (C_2H_6), and so on. In this way, a complex matrix of reactions is quickly established with a wide range of products. Such reactions are generally very fast and may be very effective in depleting old molecules or ions and in synthesizing new molecules or ions.

The ion−neutral chemistry in Titan's atmosphere is complex and has attracted the attention of chemists and astronomers. Up to now, a large number of experimental[17−27] and theoretical[28−32] studies have been performed to simulate the chemistry occurring in Titan's atmosphere. As one of the important ions in Titan's ionosphere, HCN^+ has drawn considerable attention, and many ion−molecule reactions relevant to HCN^+ have been investigated both experimentally and theoretically. In 2004, Anicich et al. performed experimental studies of HCN^+ with CH_4, C_2H_2, and C_2H_4 using the flowing after low-selected ion flow tube (FA-SIFT) at room temperature.[33] Recently, we investigated the reactions of HCN^+ with CH_4[34] and C_2H_2[35] using theoretical methods. As a part of our continuing interest in the gas-phase chemistry of HCN^+ and because there has been no theoretical study on the $HCN^+ + C_2H_4$ reaction up to now, we set out to investigate the reaction mechanism of HCN^+ with C_2H_4 in the present article.

2. Computational Methods

All calculations are performed with the *Gaussian 98* program package.[36] The geometries of all of the reactants, products, intermediates, and transition states are optimized using the popular density functional theory B3LYP[37] method (the Becke's three-parameter hybrid functional with the nonlocal correlation functional of Lee−Yang−Parr) in conjunction with the d,p-polarized 6-311G (d,p) basis set.[38−40] Frequency calculations are performed at the same level to check to see if the obtained species is an isomer or a transition state with an imaginary frequency of **0** and **1**, respectively. To get more reliable energetic data, single-point energy calculations are carried out at the CCSD(T)/6-311++G(3df,2pd)[41] level (coupled cluster approach with single and double substitutions including a perturbative estimate of connected triple substitutions) using the B3LYP/6-311G(d,p) optimized geometries. Finally, the intrinsic reaction coordinate[42] calculations are performed at the B3LYP/6-311G(d,p) level to confirm that the transition states connect designated intermediates.

Our choice of B3LYP is motivated by its good performance for the geometry optimizations and prediction of vibrational frequencies for both isomers and transition states based on much previous literature.[43−45] Moreover, B3LYP is able to suppress effectively the problem of spin contaminants. On the other hand, for the current reaction, the 6-311G(d,p) basis set is a balanced choice in consideration of computational efficiency and accuracy.

3. Results and Discussion

The optimized structures of the reactant and products are shown in Figure 1, and the optimized structures of intermediates and transition states are shown in Figures 2 and 3, respectively. The symbol **TSm/n** is used to denote the transition state connecting intermediates **m** and **n**. The energy of the reactant ($^2HCN^+ + {}^1C_2H_4$) is set to zero for reference. Unless otherwise indicated, the

10.1021/jp805285p CCC: $40.75
Published on Web 11/01/2008

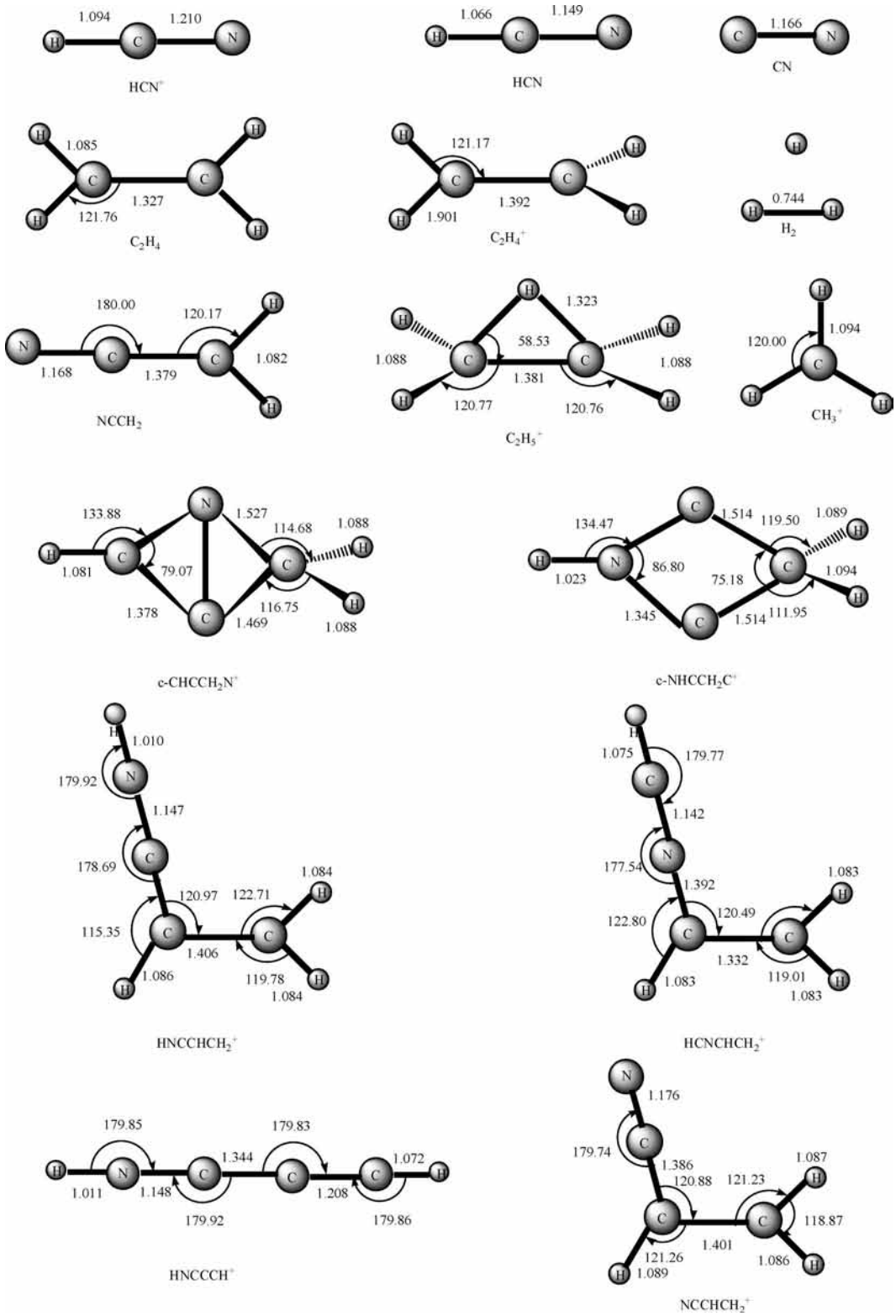

Figure 1. Optimized structures of the reactant and products. Distances are given in angstroms and angles are given in degrees.

relative energies mentioned hereafter refer to the CCSD(T)/6-311++G(3df,2pd)//B3LYP/6-311G(d,p)+ZPVE (zero-point vibrational energy) level. The energetics of the reactant and products are listed in Table 1, whereas those of the intermediates and transition states are summarized in Table 2. By means of the interrelations among the reactant, intermediates, transition states, products, and corresponding relative energies, the schematic profile of the potential energy surface (PES) for the $HCN^+ + C_2H_4$ reaction is depicted in Figure 4.

3.1. Initial Association. The reactant HCN^+ has $C_{\infty v}$ symmetry and a $^2\Sigma$ electronic state. The spin densities on carbon and nitrogen are 0.419427e and 0.594288e respectively, as confirmed by theoretical calculations at the B3LYP/6-311G(d,p) level. So, both carbon and nitrogen can be viewed as the active site of HCN^+. Via the attack of the nitrogen atom of HCN^+ at one carbon atom of C_2H_4, intermediate **1** ($HCNCH_2CH_2^+$) can be formed. Alternatively, the nitrogen atom can attack the C═C double bond of C_2H_4, and a three-membered ring intermediate **2** (HC-cN CH_2-

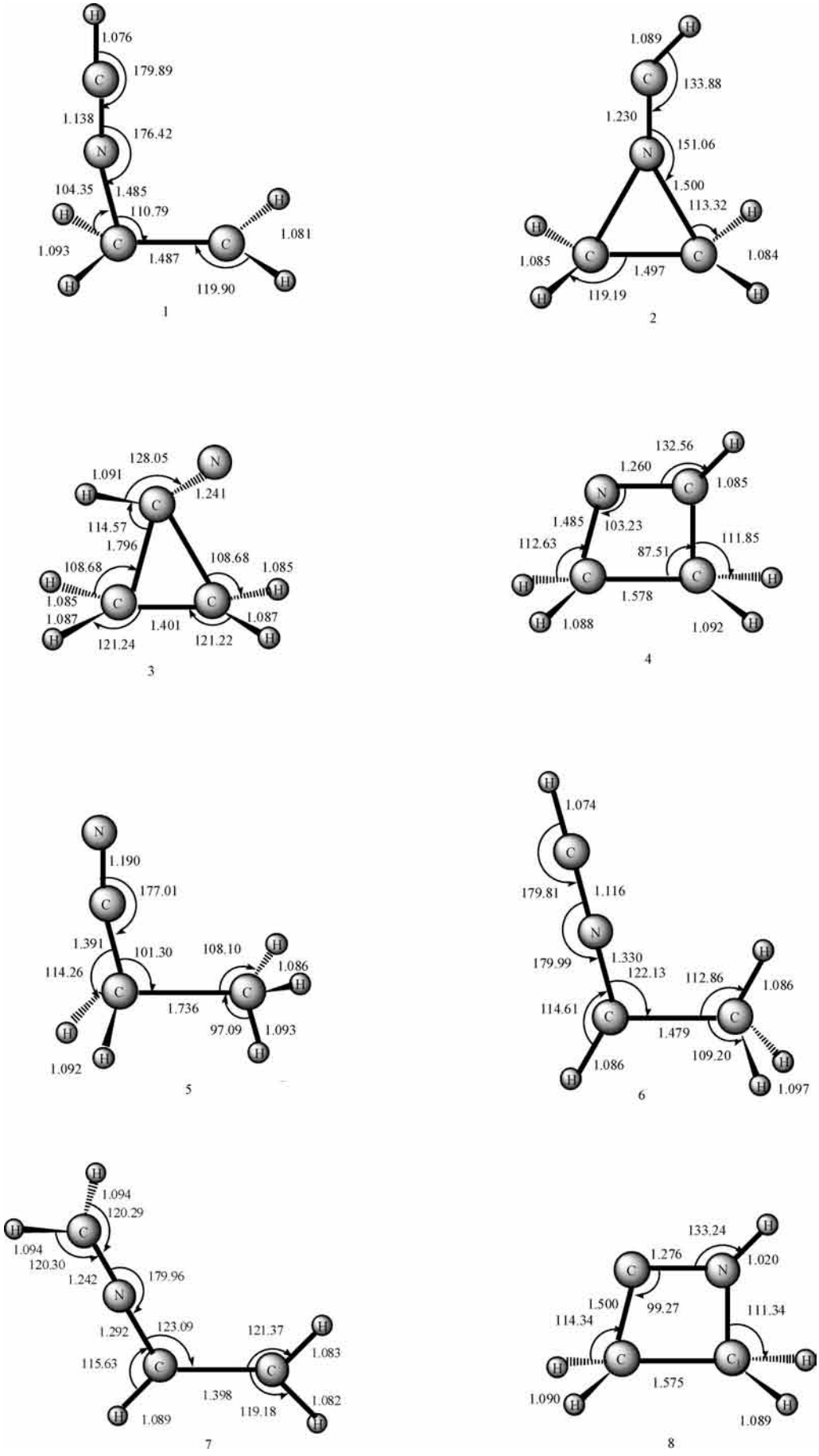

Figure 2. Part 1 of 2.

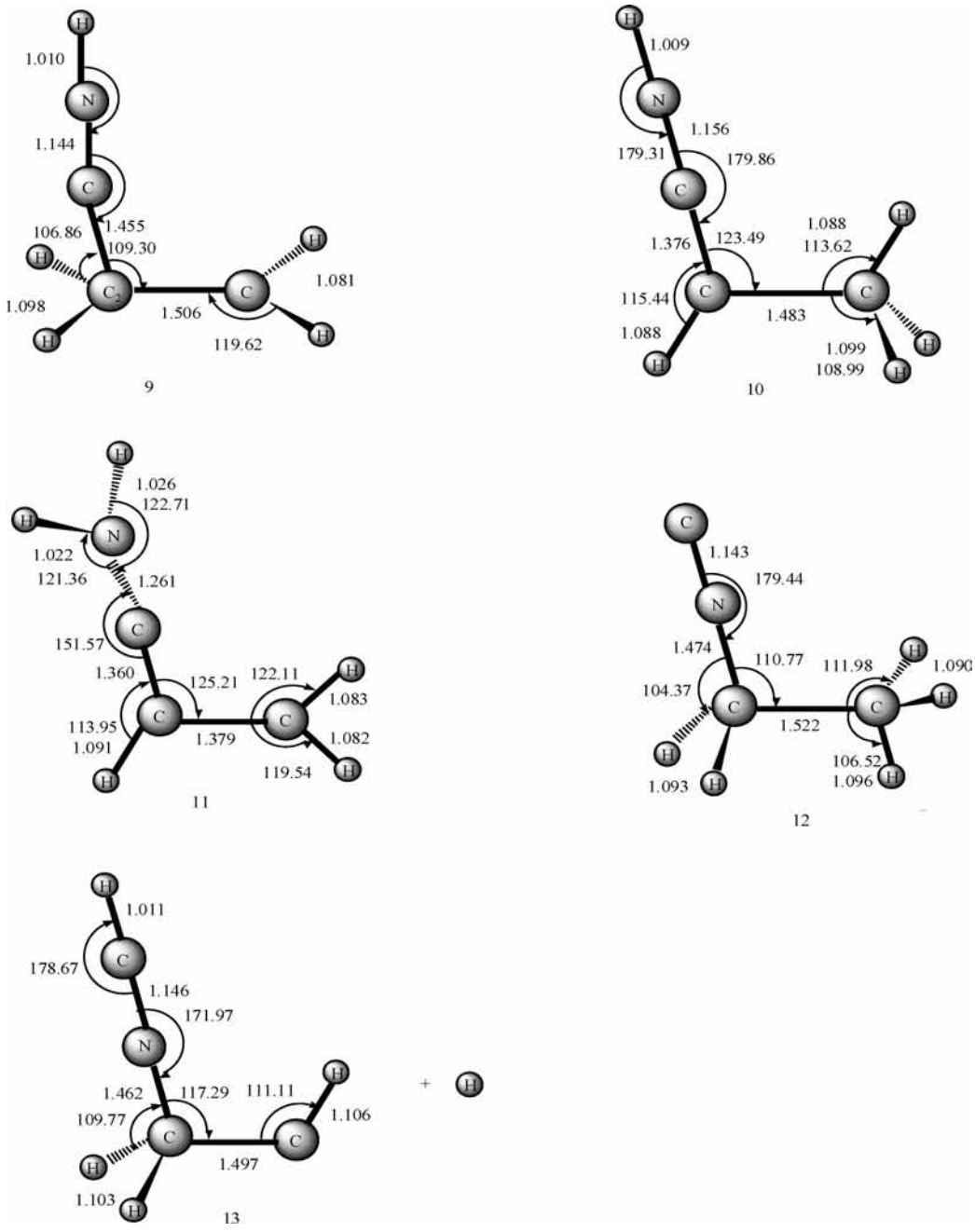

Figure 2. Part 2 of 2. Optimized structures of the intermediates. Distances are given in angstroms and angles are given in degrees.

CH_2^+) can be obtained. However, the only reaction channel from **2** is an evolution that isomerizes to the more stable intermediate **1** as shown in Figure 4. Not only can the nitrogen atom of HCN^+ attack C_2H_4, but the carbon atom in HCN^+ can also attack C_2H_4 through the two attack patterns mentioned above. Unfortunately, we cannot locate the intermediate, which can be seen as formed via the attack of one carbon of C_2H_4 by the carbon of HCN^+. However, we get a three-membered ring species **3** (N-$cCHCH_2CH_2^+$), which can be considered to form via the direct attack of the carbon atom of HCN^+ at the C═C double bond of C_2H_4. The initial adducts **1** ($HCNCH_2CH_2^+$) and **3** (N-$cCHCH_2CH_2^+$) lie 104.6 and 72.2 kcal/mol, respectively, lower in energy than reactant **R** ($HCN^+ + C_2H_4$), which means that the initial association provides the two isomers with enough energy to take subsequent isomerization or dissociation reactions. In the following passage, we mainly discuss the formation pathways of various products formed via **1** and **3**.

3.2. Isomerization and Dissociation Pathways. ***I. Reaction Product P1 (HCN + C2H4+).*** The charge-transfer product $\mathbf{P_1}$ ($HCN + C_2H_4^+$) is 70.4 kcal/mol more stable than the reactant. From Figure 4, we find that only one pathway is possible.

$$\text{Path } \mathbf{P_1}: \mathbf{R} \rightarrow \mathbf{1} \rightarrow \mathbf{P_1}$$

The initially formed intermediate **1** ($HCNCH_2CH_2^+$) can directly dissociate to $\mathbf{P_1}$ ($HCN + C_2H_4^+$) via the cleavage of the N−C single bond. At the B3LYP/6-311G(d,p) level, no transition state is found during this process ($\mathbf{1} \rightarrow \mathbf{P_1}$) in spite of numerous attempts. Alternatively, we obtain the transition state **TS1/P1** at the HF/6-311G(d,p) level, and the structure is shown in Figure 3. We attempt to reoptimize it at the MP2/6-311G(d,p) and QCISD/6-311G(d) levels. However, it does not succeed and often leads to the dissociated product $\mathbf{P_1}$. This again indicates that the dissociation of **1** to $\mathbf{P_1}$ is barrierless, and **TS1/P1** may be an artifact of the HF method.

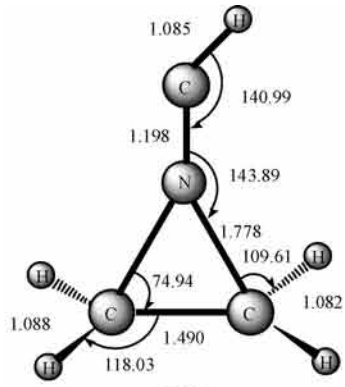

TS1/2

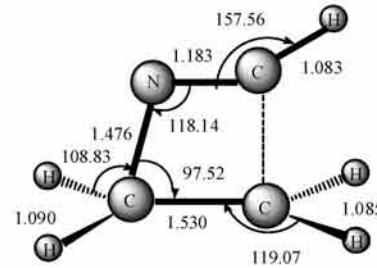

TS1/4

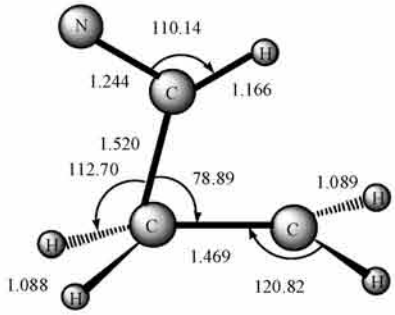

TS1/5

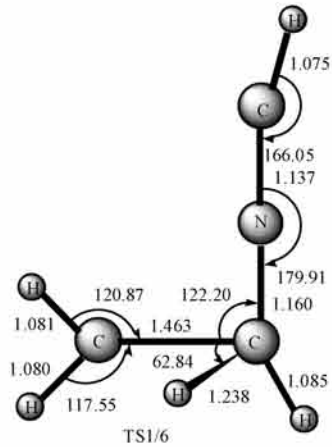

TS1/6

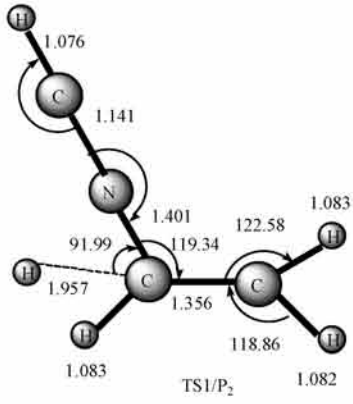

TS1/P_2

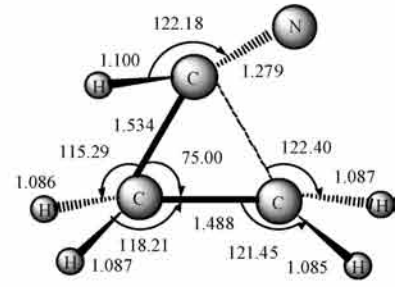

TS3/4

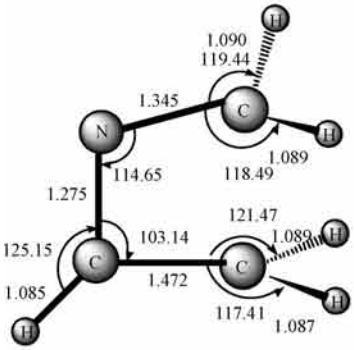

TS4/7

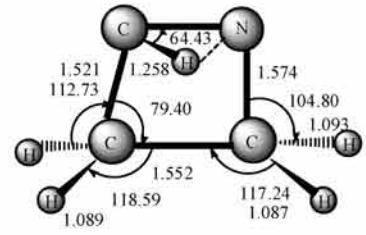

TS4/8

Figure 3. Part 1 of 3.

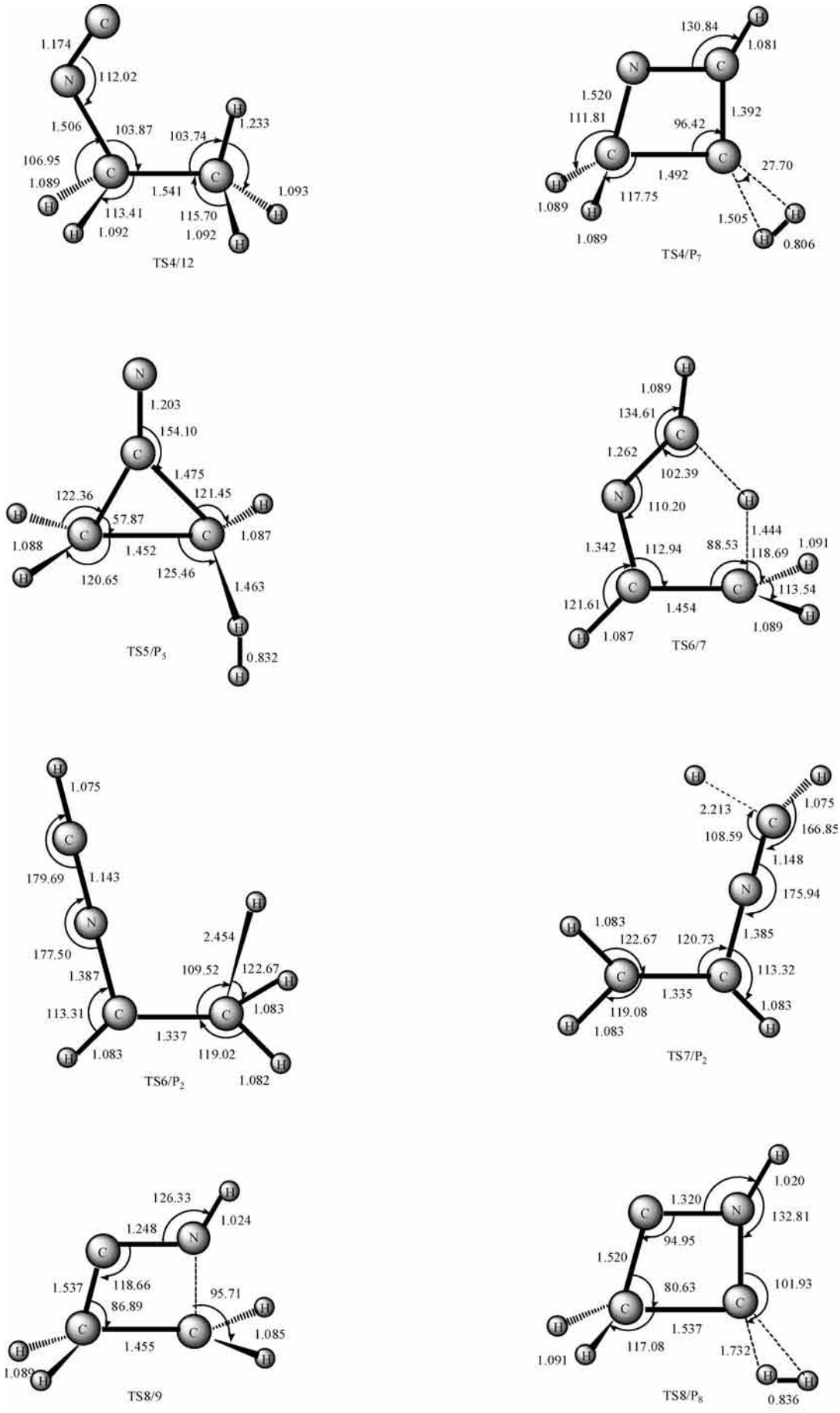

Figure 3. Part 2 of 3.

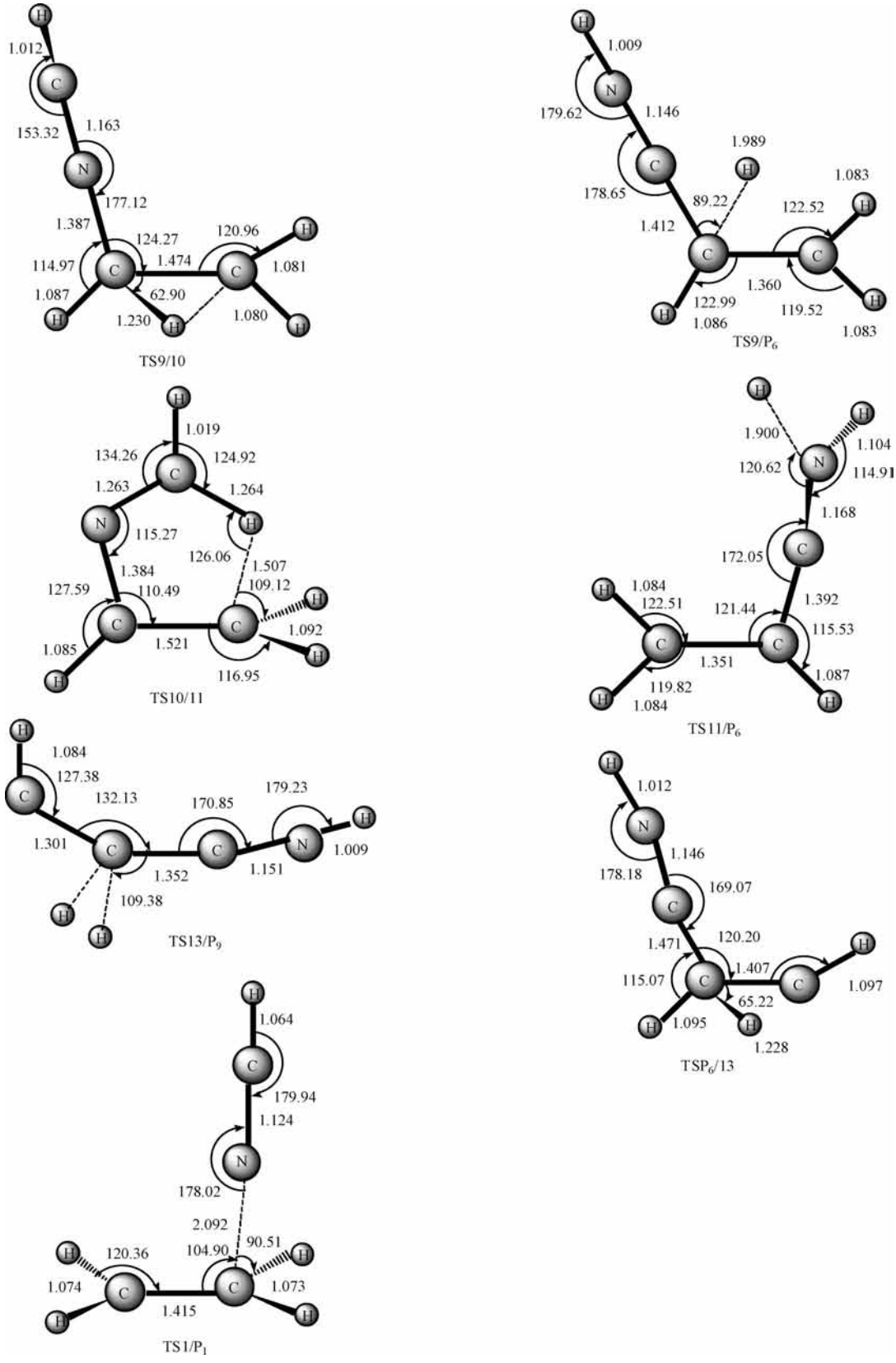

Figure 3. Part 3 of 3. Optimized structures of the transition states. Distances are given in angstroms and angles are given in degrees.

II. Reaction Product P₂ (HCNCHCH₂⁺ + H). **P₂** ($HCNCHCH_2^+ + H$) lies 70.1 kcal/mol below the reactant. From Figure 4, we find that five formation pathways are possible.

$$\text{Path } \mathbf{P_2(1)} : \mathbf{R} \rightarrow \mathbf{1} \rightarrow \mathbf{P_2}$$

$$\text{Path } \mathbf{P_2(2)} : \mathbf{R} \rightarrow \mathbf{1} \rightarrow \mathbf{6} \rightarrow \mathbf{P_2}$$

$$\text{Path } \mathbf{P_2(3)} : \mathbf{R} \rightarrow \mathbf{1} \rightarrow \mathbf{6} \rightarrow \mathbf{7} \rightarrow \mathbf{P_2}$$

$$\text{Path } \mathbf{P_2(4)} : \mathbf{R} \rightarrow \mathbf{1} \rightarrow \mathbf{4} \rightarrow \mathbf{7} \rightarrow \mathbf{P_2}$$

$$\text{Path } \mathbf{P_2(5)} : \mathbf{R} \rightarrow \mathbf{3} \rightarrow \mathbf{4} \rightarrow \mathbf{7} \rightarrow \mathbf{P_2}$$

1 ($HCNCH_2CH_2^+$) can produce **P₂** through the elimination of one of the hydrogen atoms bonded to the internal carbon as

TABLE 1: Zero-Point (kcal/mol), Total (a.u.), and Relative Energies in Parentheses (kcal/mol) and Those Including Zero-Point Vibration Energies (ZPVE) of the Reactant and Products for the $HCN^+ + C_2H_4$ Reaction

species	B3LYP	ZPVE	CCSD(T)	CCSD(T) + ZPVE
R ($^2HCN^+ + {}^1C_2H_4$)	−171.5692722	41.10053 (0.0)	−171.2177219 (0.0)	0.0
P$_1$ ($HCN + C_2H_4^+$)	−171.6871249	40.80152(−0.3)	−171.3294402 (−70.1)	−70.4
P$_2$ ($HCNCHCH_2^+ + H$)	−171.6764678	38.54916 (−2.6)	−171.3254103 (−67.6)	−70.1
P$_3$ ($NCCH_2 + CH_3^+$)	−171.6232905	39.0066 (−2.1)	−171.2315663 (−8.7)	−10.8
P$_4$ ($CN + C_2H_5^+$)	−171.6201409	40.90124 (−0.2)	−171.2730457 (−34.7)	−34.9
P$_5$ ($NCCHCH_2^+ + H_2$)	−171.670772	36.98003 (−4.1)	−171.3066598 (−55.8)	−59.9
P$_6$ ($HNCCHCH_2^+ + H$)	−171.695308	38.57216 (−2.5)	−171.3422801 (−78.2)	−80.7
P$_7$ ($c\text{-}CHCCH_2N^+ + H_2$)	−171.6057926	37.37759 (−3.7)	−171.2587270 (−25.7)	−29.5
P$_8$ ($c\text{-}NHCCH_2C^+ + H_2$)	−171.590688	37.49424 (−3.6)	−171.2417497 (−15.1)	−18.7
P$_9$ ($HNCCCH^+ + H_2 + H$)	−171.6020162	29.76482 (−11.3)	−171.2466805 (−18.2)	−29.5

TABLE 2: Zero-Point (kcal/mol), Total (a.u.), and Relative Energies in Parentheses (kcal/mol) and Those Including Zero-Point Vibration Energies (ZPVE) of the Intermediates and Transition States for the $HCN^+ + C_2H_4$ Reaction

species	B3LYP	ZPVE	CCSD(T)	CCSD(T) + ZPVE
reactant	−171.5692722	41.10053 (0.0)	−171.2177219 (0.0)	0.0
1	−171.7402572	44.08005 (3.0)	−171.3891591 (−107.6)	−104.6
2	−171.7090139	45.63058 (4.5)	−171.355261 (−86.3)	−81.8
3	−171.6920361	44.23658 (3.1)	−171.3377775 (−75.3)	−72.2
4	−171.7266609	46.24328 (5.1)	−171.3749748 (−98.7)	−93.5
5	−171.6962873	43.74696 (2.6)	−171.3345371 (−73.3)	−70.7
6	−171.763167	43.80276 (2.7)	−171.4039506 (−116.9)	−114.2
7	−171.7729872	44.84316 (3.7)	−171.417166 (−125.2)	−121.4
8	−171.7295107	47.17293 (6.1)	−171.3792192 (−101.3)	−95.3
9	−171.7556166	43.86718 (2.8)	−171.402578 (−116.0)	−113.2
10	−171.7793418	44.05545 (3.0)	−171.420203 (−127.1)	−124.1
11	−171.7665286	45.50643 (4.4)	−171.4039864 (−116.9)	−112.5
12	−171.6748028	45.68124 (4.6)	−171.3284639 (−69.5)	−64.9
13	−171.5547009	35.45405 (−5.6)	−171.2049832 (8.0)	2.3
TS1/2	−171.702453	44.27512 (3.2)	−171.3458609 (−80.4)	−77.2
TS1/4	−171.6928729	43.73375 (2.6)	−171.3392289 (−76.2)	−73.6
TS1/5	−171.6529215	42.77802 (1.7)	−171.2982557 (−50.5)	−48.9
TS1/6	−171.6911116	41.21233 (0.1)	−171.3299641 (−70.4)	−70.3
TS1/P$_2$	−171.6700632	39.49238 (−1.6)	−171.3155628 (−61.4)	−63.0
TS3/4	−171.686515	44.46459 (3.4)	−171.334576 (−73.3)	−70.0
TS4/7	−171.7002572	44.31786 (3.2)	−171.3425111 (−78.3)	−75.1
TS4/8	−171.6278185	42.68247 (1.6)	−171.2772497 (−37.4)	−35.8
TS4/12	−171.6326134	42.08896 (1.0)	−171.2784816 (−38.1)	−37.1
TS4/P$_7$	−171.6013036	39.16047 (−1.9)	−171.246473 (−18.0)	−20.0
TS5/P$_5$	−171.596166	38.13531 (−3.0)	−171.2340771 (−10.3)	−13.2
TS6/7	−171.6744336	41.808 (0.7)	−171.3162892 (−61.9)	−61.1
TS6/P$_2$	−171.6767881	38.99963 (−2.1)	−171.3236349 (−66.5)	−68.6
TS7/P$_2$	−171.6759573	39.00152 (−2.1)	−171.3209441 (−64.8)	−66.9
TS8/9	−171.6889095	44.71437 (3.6)	−171.3354826 (−73.9)	−70.3
TS8/P$_8$	−171.5775829	40.12152 (−1.0)	−171.2210284 (−2.1)	−3.1
TS9/10	−171.7133394	41.69848 (0.6)	−171.352792 (−84.8)	−84.2
TS9/P$_6$	−171.689733	39.33757 (−1.8)	−171.3335571 (−72.7)	−74.5
TS10/11	−171.6331169	40.19793 (−0.9)	−171.2682485 (−31.7)	−32.6
TS11/P$_6$	−171.6887558	39.43989 (−1.7)	−171.3276335 (−69.0)	−70.6
TS13/P$_9$	−171.4995805	32.23249 (−8.9)	−171.1384763 (49.7)	40.9
TSP$_6$/13	−171.5429315	34.54867(−6.6)	−171.1924191 (15.9)	9.3

in path **P$_2$(1)**. **1** can also isomerize into **6** ($HCNCHCH_3^+$) via a 1,2 hydrogen shift. Then **6** either undergoes a hydrogen-elimination process that leads to **P$_2$** as in path **P$_2$(2)** or continuously isomerizes into **7** ($H_2CNCHCH_2^+$) via a 1,4 hydrogen shift followed by a hydrogen-elimination process to generate **P$_2$** as in path **P$_2$(3)**. In addition, **1** can transform to the four-membered ring intermediate **4** ($c\text{-}CHCH_2CH_2N^+$) via a ring-closure process as in path **P$_2$(4)**, whereas, in path **P$_2$(5)**, **4** can be formed via **3** ($N\text{-}cCHCH_2CH_2^+$) with a negligible barrier of 2.2 kcal/mol. Subsequently, **4** undergoes a ring-opening process that gives rise to **7** ($H_2CNCHCH_2^+$) followed by a hydrogen elimination that leads to **P$_2$**.

In path **P$_2$(1)**, only one barrier of 41.6 kcal/mol needs to be overcome in order for **1** → **P$_2$** to form **P$_2$**. Yet, in path **P$_2$(2)**, there are two barriers, which are 34.7 and 45.6 kcal/mol for **1** → **6** and **6** → **P$_2$** conversions, respectively. Then we expect that path **P$_2$(1)** should be more competitive than path **P$_2$(2)**. Considering the high-energy barrier of 54.5kcal/mol for the **7** → **P$_2$** conversion that is involved in the latter three pathways, we can deduce that path **P$_2$(3)**−(**5**) cannot compete with path **P$_2$(1)**, and path **P$_2$(1)** should be the optimal channel to form **P$_2$**.

III. Reaction Product P$_3$ ($NCCH_2 + CH_3^+$). **1** ($HCN\text{-}CH_2CH_2^+$) can isomerize to **5** ($NCCH_2CH_3^+$) via a concerted 1,4 hydrogen shift, and through the −CN → −NC conversion process, the energy barrier for step **1** → **5** is 55.7 kcal/mol. Despite numerous attempts, we cannot locate the transition state for the **5** → **P$_3$** conversion; moreover, we notice that the terminal $C-C_{Me}$ (note that C_{Me} denotes the methyl carbon) bond of **5** is 1.736 Å and is easy to be broken. So, we expect that this may

be a single C−C bond-rupture process. The formation pathway of $\mathbf{P_3}$ can be written as

$$\text{Path } \mathbf{P_3}: \mathbf{R} \rightarrow \mathbf{1} \rightarrow \mathbf{5} \rightarrow \mathbf{P_3}$$

IV. Reaction Product P₄ (CN + C₂H₅⁺). For $\mathbf{P_4}$ (CN + $C_2H_5^+$), we find that two pathways are possible:

$$\text{Path } \mathbf{P_4(1)}: \mathbf{R} \rightarrow \mathbf{1} \rightarrow \mathbf{4} \rightarrow \mathbf{12} \rightarrow \mathbf{P_4}$$

$$\text{Path } \mathbf{P_4(2)}: \mathbf{R} \rightarrow \mathbf{3} \rightarrow \mathbf{4} \rightarrow \mathbf{12} \rightarrow \mathbf{P_4}$$

The formation of the four-membered ring intermediate **4** (c-$CHCH_2CH_2N^+$) has been discussed in section II. For brevity, we decide not to discuss it again. Via a hydrogen migration along with the ring-opening process, **4** can transform to **12** ($CNCH_2CH_3^+$) with a barrier of 56.4 kcal/mol followed by direct dissociation to $\mathbf{P_4}$. Because the barrier of 31.0 kcal/mol for **1** → **4** conversion is significantly higher than 2.2 kcal/mol for **3** → **4** conversion, we can deduce that path $\mathbf{P_4(2)}$ is the favorite channel to generate $\mathbf{P_4}$.

V. Reaction Product P₅ (NCCHCH₂⁺ + H₂). For product $\mathbf{P_5}$ ($NCCHCH_2^+ + H_2$), only one feasible pathway is located, which can be depicted as

$$\text{Path } \mathbf{P_5(1)}: \mathbf{R} \rightarrow \mathbf{1} \rightarrow \mathbf{5} \rightarrow \mathbf{P_5}$$

The formation of **5** ($NCCH_2CH_3^+$) is the same as path $\mathbf{P_3}$. Subsequently, **5** can produce $\mathbf{P_5}$ via a H_2 molecule elimination process. The barrier heights for the steps of **1** → **5** and **5** → $\mathbf{P_5}$ are 55.7 and 57.5 kcal/mol, respectively.

VI. Reaction Product P₆ (HNCCHCH₂⁺ + H). There are four feasible pathways to form the lowest-lying product $\mathbf{P_6}$ ($HNCCHCH_2^+ + H$), which can be written as follows:

$$\text{Path } \mathbf{P_6(1)}: \mathbf{R} \rightarrow \mathbf{1} \rightarrow \mathbf{4} \rightarrow \mathbf{8} \rightarrow \mathbf{9} \rightarrow \mathbf{P_6}$$

$$\text{Path } \mathbf{P_6(2)}: \mathbf{R} \rightarrow \mathbf{3} \rightarrow \mathbf{4} \rightarrow \mathbf{8} \rightarrow \mathbf{9} \rightarrow \mathbf{P_6}$$

$$\text{Path } \mathbf{P_6(3)}: \mathbf{R} \rightarrow \mathbf{1} \rightarrow \mathbf{4} \rightarrow \mathbf{8} \rightarrow \mathbf{9} \rightarrow \mathbf{10} \rightarrow \mathbf{11} \rightarrow \mathbf{P_6}$$

$$\text{Path } \mathbf{P_6(4)}: \mathbf{R} \rightarrow \mathbf{3} \rightarrow \mathbf{4} \rightarrow \mathbf{8} \rightarrow \mathbf{9} \rightarrow \mathbf{10} \rightarrow \mathbf{11} \rightarrow \mathbf{P_6}$$

The formation of **4** (c-$CHCH_2CH_2N^+$) has been discussed in section II. **4** can convert to **8** (c-$NHCH_2CH_2C^+$) via a hydrogen-migration process followed by a ring-opening process to give rise to **9** ($HNCCH_2CH_2^+$). The energy barriers of steps **4** → **8** and **8** → **9** are 57.7 and 25.0 kcal/mol, respectively. Subsequently, **9** can either take a hydrogen-elimination process to form $\mathbf{P_6}$ as in path $\mathbf{P_6(1)}$ and path $\mathbf{P_6(2)}$ or undergo the successive 1,2- and 1,4 hydrogen-shift interconversion to **10** ($HNCCHCH_3^+$) and then to **11** ($H_2NCCHCH_2^+$), which can finally take a direct N−H bond cleavage to give product $\mathbf{P_6}$ as in path $\mathbf{P_6(3)}$ and path $\mathbf{P_6(4)}$.

The barrier height of **1** → **4** (31.0) is much higher than that of **3** → **4** (2.2); thus, path $\mathbf{P_6(2)}$ and path $\mathbf{P_6(4)}$ are more competitive than path $\mathbf{P_6(1)}$ and path $\mathbf{P_6(3)}$, respectively. Moreover, we notice that, for **9** → $\mathbf{P_6}$ conversion, only one barrier of 38.7 kcal/mol (**9** → $\mathbf{P_6}$) must be overcome in path $\mathbf{P_6(2)}$. However, in path $\mathbf{P_6(4)}$, three barriers for **9** → **10** (39.0), **10** → **11** (91.5), and **9** → $\mathbf{P_6}$(41.9) must be overcome. So, we conclude that the optimal channel to generate $\mathbf{P_6}$ is path $\mathbf{P_6(2)}$.

VII. Reaction Product P₇ (c-CHCCH₂N⁺ + H₂). $\mathbf{P_7}$ (c-$CHCCH_2N^+ + H_2$) is a four-membered ring product, and we find two pathways are possible:

$$\text{Path } \mathbf{P_7(1)}: \mathbf{R} \rightarrow \mathbf{1} \rightarrow \mathbf{4} \rightarrow \mathbf{P_7}$$

$$\text{Path } \mathbf{P_7(2)}: \mathbf{R} \rightarrow \mathbf{3} \rightarrow \mathbf{4} \rightarrow \mathbf{P_7}$$

The four-membered ring intermediate **4** (c-$CHCH_2CH_2N^+$) can produce $\mathbf{P_7}$ via a H_2-elimination process with a barrier of 73.5 kcal/mol. Because the barrier of **3** → **4** (2.2) is much lower than that of **1** → **4** (31.0), the optimal channel to form $\mathbf{P_7}$ is path $\mathbf{P_7}$ (**2**).

VIII. Reaction Product P₈ (c-NHCCH₂C⁺ + H₂). Product $\mathbf{P_8}$ (c-$HNCCH_2C^+ + H_2$), another four-membered ring product, is 18.7 kcal/mol more stable than the reactant. From the PES, we find that two pathways are possible.

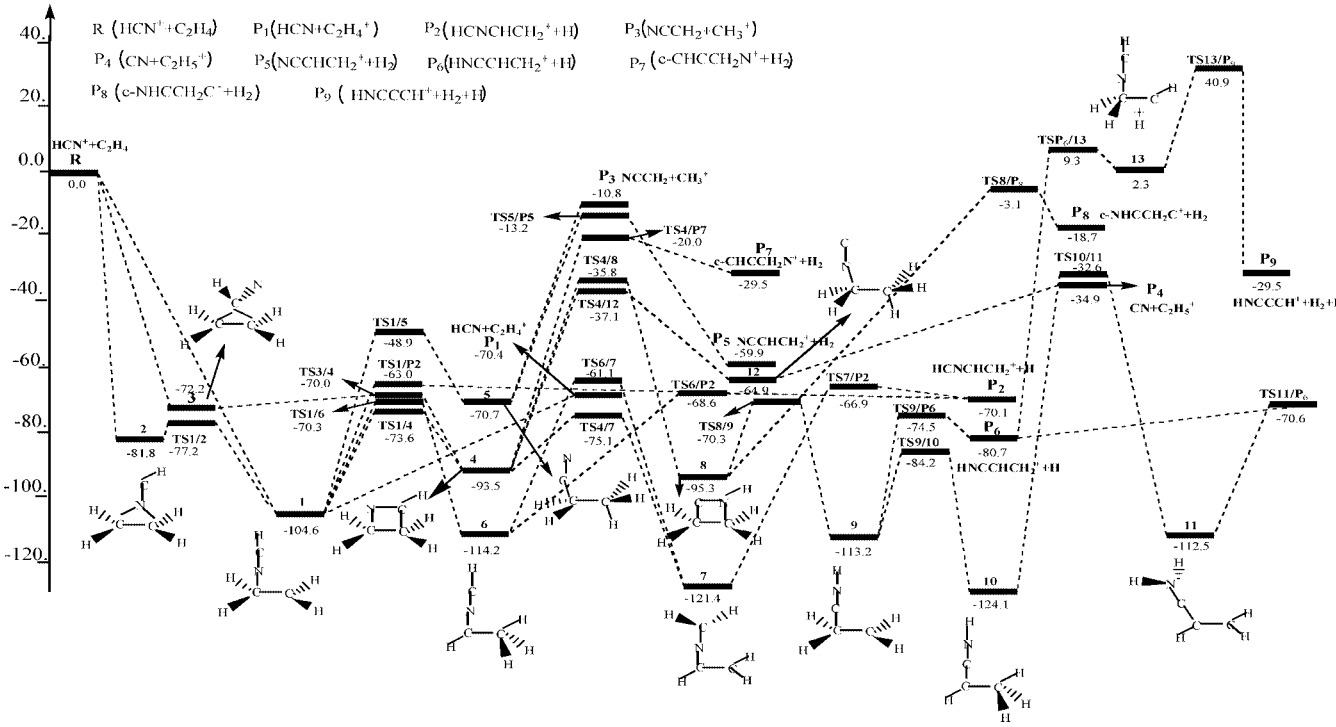

Figure 4. Sketch map of the potential energy surface (PES).

$$\text{Path } \mathbf{P_8(1)}: \mathbf{R \rightarrow 1 \rightarrow 4 \rightarrow 8 \rightarrow P_8}$$

$$\text{Path } \mathbf{P_8(2)}: \mathbf{R \rightarrow 3 \rightarrow 4 \rightarrow 8 \rightarrow P_8}$$

The formation of **8** (c-$NHCH_2CH_2C^+$) is the same as that in path $\mathbf{P_6(1)}$. Then **8** undergoes a H_2 elimination that gives rise to $\mathbf{P_8}$ with a high barrier of 92.2 kcal/mol. Comparing the energy barriers of $\mathbf{1 \rightarrow 4}$ (31.0) and $\mathbf{3 \rightarrow 4}$ (2.2), we can deduce that path $\mathbf{P_8(2)}$ is more competitive than path $\mathbf{P_8(1)}$.

IX. Reaction Product P9 ($HNCCCH^+ + H_2 + H$). $\mathbf{P_9}$ is the secondary product of $\mathbf{P_6}$. It can be formed in the following way:

$$\text{Path } \mathbf{P_9}: \mathbf{P_6 \rightarrow 13 \rightarrow P_9}$$

$\mathbf{P_6}$ is $HNCCHCH_2^+ + H$, and the way to generate it has been discussed in section VI. $\mathbf{P_6}$ can isomerize to **13** ($HNCCH_2CH^+ + H$) via a 1,2 hydrogen shift, and then **13** undergoes a H_2-elimination process that leads to $\mathbf{P_9}$. The energy barriers for $\mathbf{P_6 \rightarrow 13}$ and $\mathbf{13 \rightarrow P_9}$ are 90.0 and 38.6 kcal/mol, respectively.

3.3. Reaction Mechanism. In the preceding sections, we have obtained nine products, which are $\mathbf{P_1}$ ($HCN + C_2H_4^+$), $\mathbf{P_2}$ ($HCNCHCH_2^+ + H$), $\mathbf{P_3}$ ($NCCH_2 + CH_3^+$), $\mathbf{P_4}$ ($CN + C_2H_5^+$), $\mathbf{P_5}$ ($NCCHCH_2^+ + H_2$), $\mathbf{P_6}$ ($HNCCHCH_2^+ + H$), $\mathbf{P_7}$ (c-$CHCCH_2N^+ + H_2$), $\mathbf{P_8}$ (c-$NHCCH_2C^+ + H_2$), and $\mathbf{P_9}$ ($HNCCCH^+ + H_2 + H$). For easier discussion, the optimal channels for these nine products are listed again:

$$\text{Path } \mathbf{P_1}: \mathbf{R \rightarrow 1 \rightarrow P_1}$$

$$\text{Path } \mathbf{P_2(1)}: \mathbf{R \rightarrow 1 \rightarrow P_2}$$

$$\text{Path } \mathbf{P_3}: \mathbf{R \rightarrow 1 \rightarrow 5 \rightarrow P_3}$$

$$\text{Path } \mathbf{P_4(2)}: \mathbf{R \rightarrow 3 \rightarrow 4 \rightarrow 12 \rightarrow P_4}$$

$$\text{Path } \mathbf{P_5}: \mathbf{R \rightarrow 1 \rightarrow 5 \rightarrow P_5}$$

$$\text{Path } \mathbf{P_6(2)}: \mathbf{R \rightarrow 3 \rightarrow 4 \rightarrow 8 \rightarrow 9 \rightarrow P_6}$$

$$\text{Path } \mathbf{P_7(2)}: \mathbf{R \rightarrow 3 \rightarrow 4 \rightarrow P_7}$$

$$\text{Path } \mathbf{P_8(2)}: \mathbf{R \rightarrow 3 \rightarrow 4 \rightarrow 8 \rightarrow P_8}$$

$$\text{Path } \mathbf{P_9}: \mathbf{P_6 \rightarrow 13 \rightarrow P_9}$$

After comparing every optimal channel for forming possible products, we can deduce that the order of energy barriers of the rate-controlling steps increases as follows: path $\mathbf{P_1(1)}$ (0.0) $\rightarrow$ path $\mathbf{P_2(1)}$ (41.6) $\rightarrow$ path $\mathbf{P_3}$(55.7) $\rightarrow$ path $\mathbf{P_4(2)}$ (56.4) $\rightarrow$ path **P** (57.5) $\rightarrow$ path $\mathbf{P_6(2)}$ (57.7) $\rightarrow$ path $\mathbf{P_7(2)}$ (73.5) $\rightarrow$ path $\mathbf{P_9}$ (90.0) $\rightarrow$ path $\mathbf{P_8(2)}$ (92.2). The much higher barriers make path $\mathbf{P_7(2)}$, path $\mathbf{P_8(2)}$, and path $\mathbf{P_9}$ kinetically unfeasible. As for the remaining six channels, path $\mathbf{P_1}$ is kinetically the most favorable channel, followed by path $\mathbf{P_2(1)}$, yet it is much less competitive compared to path $\mathbf{P_1}$. Paths $\mathbf{P_{3-6}}$ are kinetically the least feasible channels. Because the energy barriers of paths $\mathbf{P_{3-6}}$ are very close, within 2 kcal/mol, these four pathways may have contributions comparable to that of the $HCN^+ + C_2H_4$ reaction. The actual yields of these four products may depend on the reaction conditions in the experiment. As a result, reflected in the final product distributions, we predict that a total of six kinds of products, $\mathbf{P_1}$ ($HCN + C_2H_4^+$), $\mathbf{P_2}$ ($HCNCHCH_2^+ + H$), $\mathbf{P_3}$ ($NCCH_2 + CH_3^+$), $\mathbf{P_4}$ ($CN + C_2H_5^+$), $\mathbf{P_5}$ ($NCCHCH_2^+ + H_2$), and $\mathbf{P_6}$ ($HNCCHCH_2^+ + H$), should be observed. $\mathbf{P_1}$ may be the most feasible product with the largest yields. $\mathbf{P_2}$ may be the second most favorable product but it is less competitive than $\mathbf{P_1}$, $\mathbf{P_3}$, $\mathbf{P_4}$, $\mathbf{P_5}$, and $\mathbf{P_6}$, which have the lowest yields observed.

4. Comparison with Experiments

In 2004, Anicich et al. performed experimental studies on the reaction $HCN^+ + C_2H_4$ using the flowing after glow-selected FA-SIFT at room temperature. The experimental results show the products and distributions are in the order of $C_2H_4^+ + HCN$ (0.73) > $H_4C_3N^+ + H$ (0.13) = $C_2H_5^+ + CN$ (0.13) > $HC_3NH^+ + H_2 + H$ (0.01). Among these products, $C_2H_4^+ + HCN$ corresponds to $\mathbf{P_1}$ in our results, and the distribution is highest in all of the products. $H_4C_3N^+ + H$ corresponds to two products in our results, which are $\mathbf{P_2}$ and $\mathbf{P_6}$. $\mathbf{P_2}$ occupies a larger part, and $C_2H_5^+ + CN$ and $HC_3NH^+ + H_2 + H$ correspond to $\mathbf{P_4}$ and $\mathbf{P_9}$, respectively. On the whole, this result is consistent with our theoretical result. However, there are some discrepancies, that is, (a) as shown in Figure 4, the relative energies of $\mathbf{P_2}$ ($HCNCHCH_2^+ + H$) and $\mathbf{P_4}$ ($CN + C_2H_5^+$) are −70.1 and −34.9 kcal/mol, respectively. In addition, energy barriers of the rate-controlling step in the formation pathways of $\mathbf{P_2}$ and $\mathbf{P_4}$ are 41.6 and 56.4 kcal/mol, respectively. Taking thermodynamics and kinetics into consideration, we believe that $H_4C_3N^+ + H$ should have a larger branching ratio than that of $C_2H_5^+ + CN$. The branching ratio of $C_2H_5^+ + CN$ obtained by Anicich et al. may be overestimated. $C_2H_5^+ + CN$ may come from another source. Notice that trace amounts of water are always present in the reaction system. As a result, H_3O^+ may react with C_2H_4 to give $C_2H_5^+$. On the other hand, dissociation of HCN and all other nitriles may yield CN radical. (b) Our calculations show that products $\mathbf{P_3}$ ($NCCH_2 + CH_3^+$) and $\mathbf{P_5}$ ($NCCHCH_2^+ + H_2$), which were completely ignored by Anicich et al., may also contribute to the final products. The absence of a measurable signal in these cases cannot be taken as proof of the insignificance of these possible products in the reaction $HCN^+ + C_2H_4$ because the sensitivity of their experimental system is not known for these species. Moreover, the existence of $NCCH_2$ and $NCCHCH_2^+$ in interstellar space has been suggested by previous studies.[46,47] Therefore, further experimental investigation is still desirable.

The energies of the reactant, products, intermediates, and transition states may be different at different temperatures. From Figure 4, we find that most of the pathways on the PES are exothermic channels, and an increase in temperature may make it easier to proceed through these channels. However, considering that the low temperature in Titan's atmosphere is about 170 K, and its surface temperature is 96 K,[48] the energy correction for temperature (from 0 to 170 K) may not play a large role.

5. Conclusions

A detailed doublet PES of the $HCN^+ + C_2H_4$ reaction system is built up at the B3LYP and CCSD(T) (single-point) levels of theory. The main calculated results can be summarized as follows: The reaction initiated by the formation of three minimal isomers **1**, **2**, and **3** followed by a variety of transformations lead to nine dissociation products. Among the nine products, the charge-transfer product $\mathbf{P_1}$ ($C_2H_4^+ + HCN$) is the most favorable product; $\mathbf{P_2}$ ($HCNCHCH_2^+ + H$) is the second most feasible product but it is much less competitive than $\mathbf{P_1}$; and $\mathbf{P_3}$ ($NCCH_2 + CH_3^+$), $\mathbf{P_4}$ ($CN + C_2H_5^+$), $\mathbf{P_5}$ ($NCCHCH_2^+ + H_2$), and $\mathbf{P_6}$ ($HNCCHCH_2^+ + H$) make up the third most feasible products, yet they are much less competitive than $\mathbf{P_1}$ and $\mathbf{P_2}$. Other products, namely, $\mathbf{P_7}$ (c-$CHCCH_2N^+ + H_2$), $\mathbf{P_8}$ (c-$HNCCH_2C^+ + H_2$), and $\mathbf{P_9}$ ($HNCCCH^+ + H_2 + H$), are kinetically unfavorable, and their contribution to the final products can be considered negligible. Because the isomers and transition states involved in the most favorable channel of the $HCN^+ + C_2H_4$ reaction are lower in energy than the reactant, the total reaction is expected to be rapid, as is confirmed by experiment. Our theoretical results are consistent with the experimental investigations, and we hope the results may provide

some useful information for understanding the reaction mechanism of HCN^+ with unsaturated hydrocarbon.

Acknowledgment. This work was supported by the National Natural Science Foundation of China (Grant 20773048).

References and Notes

(1) Sagan, C.; Thompson, W. R. *Icarus* **1984**, *59*, 133.
(2) Cousteins, A.; Encrenaz, T.; Bézard, B. *Icarus* **1993**, *102*, 240.
(3) Keller, C. N.; Cravens, T. E.; Gan, L. *J. Geophys. Res.* **1992**, *97*, 12117.
(4) Lara, L. M.; Lellouch, E.; Loppez-Moreno, J. J.; Rodrigo, R. *J. Geophys. Res., [Atmos.]* **1996**, *97*, 12261.
(5) Toublanc, D.; Parisot, J. P.; Brillet, J.; Gautier, D.; Raulin, F.; Mckay, C. P. *Icarus* **1995**, *113*, 2.
(6) Yung, Y. L.; Allen, M.; Pinto, J. P. *Astrophys. J.* **1984**, *55*, 465.
(7) Bauer, S. J. *Adv. Space Res.* **1987**, *7*, 65.
(8) Cravens, T. E.; Robertson, I. P.; Waite, J. H.; Yelle, R. V.; Kasprzak, W. T.; Keller, C. N.; Ledvina, S. A.; Niemann, H. B.; Luhmann, J. G.; McNutt, R. L.; Ip, W. H.; DeLaHaye, V.; Mueller-Wodarg, I.; Wahlund, J. E.; Anicich, V. G.; Vuitton, V. *Geophys. Res. Lett.* **2006**, *33* (7), Art. No. L07105.
(9) Fulchignoni, M.; Ferri, F.; Angrilli, F.; Ball, A. J.; Bar-Nun, A.; Barucci, M. A.; Bettanini, C.; Bianchini, G.; Borucki, W.; Colombatti, G.; Coradini, M.; Coustenis, A.; Debei, S.; Falkner, P.; Fanti, G.; Flamini, E.; Gaborit, V.; Grard, R.; Hamelin, M. M.; Harri, A.; Hathi, B.; Jernej, I.; Leese, M. R.; Lehto, A.; Lion Stoppato, P. F.; López-Moreno, J. J.; Mäkinen, T.; McDonnell, J. A. M.; McKay, C. P.; Molina-Cuberos, G.; Neubauer, F. M.; Pirronello, V.; Rodrigo, R.; Saggin, B.; Schwingenschuh, K.; Seiff, A.; Simões, F.; Svedhem, H.; Tokano, T.; Towner, M. C.; Trautner, R.; Withers, P.; Zarnecki, J. C. *Nature* **2006**, *438*, 785.
(10) Broadfoot, A.; Sandel, B.; Shemansky, D.; Holberg, J.; Smith, G.; Strobel, D.; McConnell, J.; Kumar, S.; Hunten, D.; Atreya, S.; Donahue, T.; Moos, H.; Bertaux, J.; Blamont, J.; Pomphrey, R.; Linick, S. *Science* **1981**, *212*, 206.
(11) Hanel, R.; Conrath, B.; Flasar, F.; Kunde, V.; Maguire, W.; Pearl, J.; Pirraglia, J.; Samuelson, R.; Herath, L.; Allison, M.; Cruikshank, D.; Gautier, D.; Gierasch, P.; Horn, L.; Koppany, R.; Ponnamperuma, C. *Science* **1981**, *212*, 192.
(12) Samuelson, R.; Nath, N.; Borysow, A. *Planet. Space Sci.* **1997**, *45*, 959.
(13) Cravens, T. E.; Keller, C. N.; Gan, L. Proceedings of the Symposium on Titan; ESA: 1992; SP-338, 273.
(14) Banaskiewicz, M.; Lara, M. L.; Rodrigo, R.; López-Moreno, J. J.; Molina-Cuberos, G. J. *Icarus* **2000**, *147*, 386.
(15) Wahlund, J. E.; Boström, R.; Gustafsson, G.; Gurnett, D. A.; Kurth, W. S.; Pedersen, A.; Averkamp, T. F.; Hospodarsky, G. B.; Personn, A. M.; Canu, P.; Neubauer, F. M.; Dougherty, M. K.; Eriksson, A. I.; Morooka, M. W.; Gill, R.; André, M.; Eliasson, L.; Müller-Wodarg, I. *Science* **2005**, *308*, 986.
(16) Lilensten, J.; Simon, C.; Witasse, O.; Dutuit, O.; Thissen, R.; Alcaraz, C. *Icarus* **2005**, *174*, 285.
(17) Anicich, V. G.; Milligan, D. B.; Fairley, D. A.; McEwan, M. J. *Icarus* **2000**, *146*, 118.
(18) Anicich, V. G.; Wilson, P. F.; McEwan, M. J. *J. Am. Soc. Mass Spectrom.* **2003**, *14*, 900.
(19) Anicich, V. G.; Wilson, P. F.; McEwan, M. J. *J. Am. Soc. Mass Spectrom.* **2004**, *15*, 1148.
(20) Anicich, V. G.; McEwan, M. J. *J. Am. Soc. Mass Spectrom.* **2006**, *17*, 544.
(21) Adames, N.; Smith, D. *J. Am. Soc. Mass Spectrom.* **1976**, *21*, 349.
(22) Adames, N.; Smith, D. *J. Chem. Phys.* **1980**, *72*, 288.
(23) Dobrijevic, M.; Ollivier, J. L.; Billebaud, F.; Brillet, J.; Parisot, J. *Acta Astronaut.* **2003**, *398*, 335.
(24) Smith, D.; Adames, N.; Miller, T. *J. Chem. Phys.* **1978**, *69*, 308.
(25) Toublanc, D.; Parisot, J.; Briller, J.; Gautier, D.; Raulin, F.; Mckay, C. *Icarus* **1995**, *113*, 2.
(26) Alcaraz, C.; Nicolas, C.; Thissen, R.; Zabka, J.; Dutuit, O. *J. Phys. Chem. A* **2004**, *108*, 9998.
(27) Sekine, Y.; Imanaka, H.; Matsui, T.; Khare, B. N.; Bakes, E. L. O.; Mckay, C. P.; Sugita, S. J. *Icarus* **2008**, *194*, 186.
(28) Redondo, P.; Pauzat, F.; Ellinger, Y. *Planet. Space Sci.* **2006**, *54*, 181.
(29) Marco, D. S.; Marzio, R.; Antonio, S. *Chem. Phys.* **2004**, *297*, 121.
(30) Alves, T. V.; de Oliveria, A. G. S.; Ornellas, F. S. *Chem. Phys. Lett.* **2008**, *457*, 36.
(31) Milligan, D. B.; Freeman, C. G.; Maclagan, R. G. A. R.; McEwan, M. J.; Wilson, P. F.; Anicich, V. G. *J. Am. Soc. Mass Spectrom.* **2001**, *12*, 557.
(32) Osamura, Y.; Petrie, S. *J. Phys. Chem. A* **2004**, *108*, 3615.
(33) Anicich, V. G.; Wilson, P. F.; McEwan, M. J. *J. Am. Soc. Mass Spectrom.* **2004**, *15*, 1148.
(34) Li, Y.; Liu, H. L.; Huang, X. R.; Geng, C. Y.; Sun, C. C.; Tang, A. C. *J. Phys. Chem. A* **2008**, *112*, 2693.
(35) Li, Y.; Liu, H. L.; Huang, X. R.; Wang, D. Q.; Sun, C. C.; Tang, A. C. *J. Phys. Chem. A* **2008**, *112*, 8188.
(36) Frisch, M. J.; Trucks, G. W.; Schlegel, H. B.; et al. *Gaussian 98*, Revision A.6; Gaussian, Inc.: Pittsburgh, PA, 1998.
(37) Becke, A. D. *J. Chem. Phys.* **1993**, *98*, 5648.
(38) McLean, A. D.; Chandler, G. S. *J. Chem. Phys.* **1980**, *72*, 5639.
(39) Krishnan, R.; Binkley, J. S.; Seeger, R.; Pople, J. A. *J. Chem. Phys.* **1980**, *72*, 650.
(40) Frisch, M. J.; Pople, J. A.; Binkley, J. S. *J. Chem. Phys.* **1984**, *80*, 3265.
(41) Pople, J. A.; Head-Gordon, M.; Raghavachari, K. *J. Chem. Phys.* **1987**, *87*, 5968.
(42) (a) Gonzalez, C.; Schlegel, H. B. *J. Chem. Phys.* **1989**, *90*, 2154. (b) Gonzalez, C.; Schlegel, H. B. *J. Chem. Phys.* **1990**, *94*, 5523.
(43) (a) The performance of the B3LYP functional for geometry optimization was assessed, for example, by the authors of several versatile model chemistries. G2(B3LYP/MP2/CC): Bauschlicher, C. W.; Partridge, H. *J. Chem. Phys.* **1995**, *103*, 1788. (b) G2M: Mebel, A. M.; Morokuma, K.; Lin, M. C. *J. Chem. Phys.* **1995**, *103*, 7414. (c) G3//B3LYP: Baboul, A. G.; Curtiss, L. A.; Redfern, P. C.; Raghavachari, K. *J. Chem. Phys.* **1999**, *110*, 7650. (d) G3X: Curtiss, L. A.; Redfern, P. C.; Raghavachari, K.; Pople, J. A. *J. Chem. Phys.* **2001**, *114*, 108.
(44) Tokmakov, I. V.; Lin, M. C. *J. Phys. Chem. A* **2002**, *106*, 11309.
(45) Xie, H. B.; Ding, Y. H.; Sun, C. C. *J. Theor. Comput. Chem.* **2005**, *4*, 1029.
(46) Nesbitt, F. L.; Marston, G.; Stief, L. J. First International Conference on Laboratory Research for Planetary Atmospheres; pp 244−248.
(47) Manaszkiewicz, M.; Lara, L. M.; Rodrigo, R.; López-Moreno, J. J.; Molina-Cuberos, G. J. *Icarus* **2000**, *147*, 386.
(48) Mousis, O.; Gautier, D.; Coustenis, A. *Icarus* **2002**, *159*, 156.

JP805285P